

This document is confidential and is proprietary to the American Chemical Society and its authors. Do not copy or disclose without written permission. If you have received this item in error, notify the sender and delete all copies.

Heat Capacity of Saturated and Compressed Liquid Dimethyl Ether at Temperatures from (132 to 345) K and at Pressures to 35 MPa

Journal:	<i>Journal of Chemical & Engineering Data</i>
Manuscript ID	je-2018-00037v.R1
Manuscript Type:	Article
Date Submitted by the Author:	n/a
Complete List of Authors:	Wu, Jiangtao; Xi'an Jiaotong University, Center of Thermal and Fluid Science; Xi'an Jiaotong University, Center of Thermal and Fluid Science Magee, Joseph; NIST 838.01, ;

SCHOLARONE™
Manuscripts

1
2
3 **Heat Capacity of Saturated and Compressed Liquid Dimethyl Ether at Temperatures from**
4
5 **(132 to 345) K and at Pressures to 35 MPa**
6

7 Jiangtao Wu^{1,2} and Joseph W. Magee^{1,3}
8
9

10
11
12
13
14
15
16
17
18
19 A contribution of the National Institute of Standards and Technology, not subject to copyright in
20
21 the U.S.
22
23
24
25
26
27
28
29
30
31
32
33
34
35
36

37
38 ¹ Thermodynamics Research Center, Applied Chemicals and Materials Division (647), Material
39
40 Measurement Laboratory, National Institute of Standards and Technology, Boulder, Colorado
41
42 80305-3337, USA.
43

44
45 ² Present address: Xi'an Jiaotong University, Xi'an, Shaanxi, 710049 People's Republic of
46
47 China.
48

49 ³ To whom correspondence should be addressed.
50
51
52
53
54
55
56
57
58
59
60

ABSTRACT

Molar heat capacities at constant volume (C_v) of dimethyl ether have been measured with an adiabatic calorimeter. Temperatures range from the triple point to 345 K, and pressures up to 35 MPa. Measurements were conducted on liquid in equilibrium with its vapor and on compressed liquid samples. The samples are of high purity, as verified by chemical analysis. Calorimetric quantities are reported for the two-phase ($C_v^{(2)}$), saturated-liquid (C_σ or C_x'), and single-phase (C_v) molar heat capacities. Low temperature $C_v^{(2)}$ data were employed to estimate vapor pressures for values less than 340 kPa by applying a thermodynamic relationship between the two-phase internal energy $U^{(2)}$ and the temperature derivatives of the vapor pressure. Vapor pressures were calculated at temperatures as low as the triple-point temperature. The principal sources of uncertainty are the temperature rise measurement and the change-of-volume work adjustment. The expanded relative uncertainty (with a coverage factor $k=2$ and thus a two-standard deviation estimate) is estimated to be 0.7 % for C_v , 0.5 % for $C_v^{(2)}$ and 0.7 % for C_σ .

1. INTRODUCTION

Thermodynamic properties of a fluid may be calculated from a knowledge of its ideal-gas properties and an accurate equation of state. Heat capacities derived in this manner, however, often lack sufficient accuracy since the calculation involves integration of the isochoric curvature $(\partial^2 p / \partial T^2)_\rho$ as in the thermodynamic relation,

$$C_v - C_v^0 = -T \int_0^\rho \left(\frac{\partial^2 p}{\partial T^2} \right)_\rho \frac{d\rho}{\rho^2} \quad (1)$$

where C_v^0 is the ideal-gas heat capacity. Since $(\partial^2 p / \partial T^2)_\rho$ possesses small absolute values, except in the vicinity of the critical point, it is very difficult to measure accurately. To calculate C_v for compressed liquid states, additional data are required, including the vapor pressure and enthalpy of vaporization or heat capacity of the saturated liquid. Direct measurements of heat capacities will provide useful checks on calculated heat capacities when they are available along a path traversing the temperature range of interest. In many cases, such data are scarce.

In two recent manuscripts, Ihmels and Lemmon [1] and Wu *et al.* [2] reviewed published thermodynamic property measurements for dimethyl ether. Only five other sources of heat capacity data for dimethyl ether were found, and all five sources report values of heat capacity at constant pressure C_p . Just one of these studies reported saturated liquid heat capacities, and taken individually, each study covers a limited temperature range. As shown by $\pm 8\%$ deviations from their equation of state depicted in Figure 17 of Ref. [2], the five sources of C_p do not display mutual agreement. This finding makes it clear why another reliable set of heat capacity measurements, spanning a wide range of temperature, would have a positive impact on an equation of state model.

Both reviews mentioned above [1,2] include a detailed review of the thermodynamic

1
2
3 property literature and show the development of an equation of state model. Ref. [1] also
4
5 presents new experimental data for vapor pressure and density in wide ranges of temperature and
6
7 pressure. Both reviews have important connections to the present study. The first review by
8
9 Ihmels and Lemmon [1] was done before the present work; hence, it does not include the
10
11 experimental data from this study. The second review by Wu *et al.* [2] does include all the
12
13 present experimental data. In our numerical data comparisons in this work, we have used only
14
15 the Ihmels and Lemmon model for calculations of heat capacity, vapor pressure and density. In
16
17 this way, we will show meaningful comparisons with a model that's based solely on prior
18
19 studies. For very detailed comparisons of thermodynamic data (circa 2011), including the present
20
21 results, we would recommend consulting the review of Wu *et al.* [2].
22
23
24
25

26 In this paper, heat capacity and density data are reported for the compressed liquid region
27
28 and the saturated liquid region from near the triple-point temperature to the upper limit (345 K)
29
30 of the apparatus. In addition, vapor pressures evaluated from two-phase heat capacity
31
32 measurements are reported from the triple point temperature to the normal boiling point
33
34 temperature.
35
36

37 **2. MEASUREMENTS**

38 **2.1. Apparatus and Procedures**

39
40
41 The calorimeter used for these measurements has been described in detail by Goodwin
42
43 [3] and Magee [4]. A spherical bomb contains a sample of known mass. The volume of the
44
45 bomb, approximately 78 cm³, is a function of temperature and pressure. A platinum resistance
46
47 thermometer is attached to the bomb for the temperature measurement. Temperatures are
48
49 reported on the ITS-90, after conversions from the original calibration on the IPTS-68. Pressures
50
51 are measured with an oscillating quartz crystal pressure transducer with a 0 to 70 MPa range.
52
53
54
55
56
57
58
59
60

1
2
3 Adiabatic conditions are ensured by a high vacuum (3×10^{-3} Pa) in the can surrounding the
4 bomb, by a temperature-controlled radiation shield, and by a temperature-controlled guard ring
5 which thermally anchors the filling capillary and the lead wires to the bomb.
6
7

8
9
10 For the heat-capacity measurement, a precisely determined electrical energy (Q) is
11 applied and the resulting temperature rise ($\Delta T = T_2 - T_1$) is measured. We obtain the heat
12 capacity from
13
14

$$15 \quad C_v = \left(\frac{\partial U}{\partial T}\right)_v \cong \frac{Q - Q_0 - W_{pV}}{n\Delta T} \quad (2)$$

16
17 where U is the internal energy, Q_0 is the energy required to heat the empty calorimeter, W_{pV} is
18 the change-of-volume work that results from the slight dilation of the bomb, and n is the number
19 of moles enclosed in the bomb. To set up this work, the bomb was initially charged with sample
20 up to the highest filling density. The bomb and its contents were cooled to a starting temperature
21 in the single-phase region. Measurements were then performed in that region with increasing
22 temperature until either the upper temperature (345 K) or pressure limit (35 MPa) was attained.
23 For two different filling densities, the bomb was then cooled to a temperature inside the
24 two-phase region, and measurements were carried out on a two-phase sample. At the completion
25 of a run, a small part of the sample was cryopumped into a lightweight cylinder and weighed
26 ($u(w) = 5 \times 10^{-4}$ g) after applying a buoyancy correction. The next run was started with a smaller
27 density. All data points were measured from a single filling of the calorimetric bomb. After the
28 last run was completed, the remaining sample was discharged and weighed ($u(w) = 5 \times 10^{-3}$ g),
29 again, after applying a buoyancy correction.
30
31
32
33
34
35
36
37
38
39
40
41
42
43
44
45
46
47
48
49

50
51 A series of such runs with different fillings constitutes the investigation of the (p , T , C_v)
52 surface. The ranges of temperature and pressure were predetermined to cover primarily the
53
54
55
56
57
58
59
60

1
2
3 liquid-phase region for dimethyl ether. Within these ranges, C_v measurements were performed on
4
5 nine isochores for 117 state conditions at (158 to 344) K and (2.5 to 33.8) MPa. The two-phase
6
7 heat capacity (leading to C_σ) measurements followed the path of (p,T) states defined by the
8
9 vapor-pressure curves. For dimethyl ether, 90 two-phase points were measured at temperatures
10
11 from (133 to 345) K.
12
13

14 15 **2.2. Samples**

16
17 A commercial vendor supplied a fractionally-distilled sample of dimethyl ether with a
18
19 stated purity of 0.999 mole fraction. In house gas chromatography-mass spectrometry testing
20
21 validated the vendor's purity claim. The sample was used as received without further
22
23 purification.
24
25

26 27 **3. RESULTS**

28 29 **3.1. Heat Capacity**

30
31 A search of the literature disclosed the following. Six sources of heat capacity
32
33 measurements at constant pressure (C_p) were found. No published C_v data were found. Jatkar [5]
34
35 reported C_p measurements at two temperatures $T = 298$ K and 370 K and at pressures of 99 kPa
36
37 and 101 kPa, respectively. Kistiakowsky and Rice [6] have reported C_p measurements at four
38
39 temperatures from (272 to 370) K and at a pressure of 100 kPa. Kennedy *et al.* [7] reported 32 C_p
40
41 measurements at temperatures from (137 to 245) K and at saturated liquid pressures. Miyazaki *et*
42
43 *al.* [8] reported 12 C_p measurements at temperatures from (303 to 343) K and at pressures from
44
45 (200 to 500) kPa. Tanaka and Higashi [9] reported 29 C_p measurements for dimethyl ether at
46
47 temperatures from (310 to 320) K and at pressures from (2 to 5) MPa. Lastly, He *et al.* [10]
48
49 reported 81 C_p measurements for dimethyl ether at temperatures from (305 to 365) K and at
50
51 pressures from (1.5 to 5) MPa. This last study was published in 2014. Since He *et al.* results were
52
53
54
55
56
57
58
59
60

not used to develop the model of Wu *et al.* [2] (in 2011), these C_p measurements should be useful to validate this model, and by proxy, the liquid-phase measurements of this work, which were fitted by Wu *et al.* In addition, the Kennedy *et al.* [7] measurements of both C_p and vapor pressure should be useful for direct comparisons with this work on the vapor-liquid saturation boundary.

As mentioned in Section 2.1, adjustments should be applied to the raw heat-capacity data for the change-of-volume work of the bomb. During a measurement sequence, the volume of the bomb varies with temperature and pressure in accordance with formulas reported previously [4]. It is an important adjustment since the bomb is thin-walled. Referring to Goodwin and Weber [11], we can obtain the work from

$$W_{pV} = (T_2 \left(\frac{\partial p}{\partial T} \right)_{V_2} - \frac{1}{2} \Delta p) \Delta V \quad (3)$$

where $\Delta p = p_2 - p_1$ is the pressure rise and $\Delta V = V_2 - V_1$ is the change of volume. The pressure derivative is calculated from an equation of state. Precise values for the pressure derivative were required, since this quantity can have a significant influence on the adjustment for the change-of-volume work. This derivative was calculated with a fundamental equation of state reported by Ihmels and Lemmon [1].

The heat-capacity data of each run are presented in Table 1 for two-phase states, and in Table 2 for single-phase states. The average of the initial and final temperatures T_{avg} of each heating interval is given for the data point temperature (ITS-90). Experimentally, we observed an average temperature rise of approximately 2 °C. In Table 2, the average pressures P_{avg} were calculated at T_{avg} by using our least-squares fit to the (P, T) measurements recorded on each isochore. For least-squares fitting of pressure as a function of temperature, we used a 7-term equation form we adopted from Jacobsen and Stewart [12], which was used in their equation of

1
2
3 state. In Table 1 for the two-phase region, however, most of the measured vapor pressures are
4 below the accurate range of the pressure gauge (3 to 70) MPa. Thus, the pressures were
5 calculated from a vapor-pressure equation [1] and are presented as calculated values in the Table
6
7
8
9
10
11
12
13
14
15
16
17
18
19
20
21
22
23
24
25
26
27
28
29
30
31
32
33
34
35
36
37
38
39
40
41
42
43
44
45
46
47
48
49
50
51
52
53
54
55
56
57
58
59
60

1. The density, given in Table 2 for single-phase states, is calculated from the corrected number of moles and the bomb volume. Our experimental densities have an estimated relative expanded uncertainty of 0.2 %. While they are not the primary result of our study, they could be used as supplementary information on the thermodynamic properties of dimethyl ether. Table 3 presents a comparison of measured liquid densities with those that were calculated with the Ihmels and Lemmon [1] equation of state, which was published prior to this study; we observe a maximum deviation of just 0.18 %. Considering that none of our densities were used to fit the model in Ref. [1], we find this to be a satisfactory level of agreement between our study and this model. This result lends additional confidence to our experimental measurements of sample mass and calorimeter volume.

In Table 1, values of the two-phase heat capacity at constant volume ($C_v^{(2)}$) are presented as well as values of the saturated-liquid heat capacity C_σ [described by some authors as $C_x' = T(dS' / dT)$]. Values of C_σ are obtained by adjusting $C_v^{(2)}$ data with a relation given by Rowlinson [13]

$$C_\sigma = C_v^{(2)} - \frac{T}{\rho^2} \left(\frac{d\rho}{dT} \right)_\sigma \left(\frac{dp}{dT} \right)_\sigma + T \left(\frac{1}{\rho_\sigma} - \frac{1}{\rho} \right) \frac{d^2 p_\sigma}{dT^2} \quad (4)$$

where ρ_σ and p_σ are the density and the pressure of the saturated liquid and ρ is the bulk density of the sample residing in the bomb. The derivative quantities were calculated with the ancillary equations of Ihmels and Lemmon [1].

The saturated-liquid heat capacity C_σ , as a saturation quantity, depends only on

1
2
3 temperature. We will take advantage of the univariant behavior to compare directly with
4 published measurements; there is just one data set by Kennedy *et al.* [7] who measured $C_{p,\sigma}$ close
5 to the vapor pressure conditions of (1 to 101) kPa. Furthermore, since the Kennedy *et al.*
6 pressures are quite low, we do not need to transform $C_{p,\sigma}$ to C_σ ; rather we could take advantage
7 of the approximation $C_{p,\sigma} \cong C_v^{(2)} \cong C_\sigma$ which is valid at low pressure on the saturated liquid curve.
8 The saturated liquid heat capacities for this work and for Kennedy *et al.* are depicted graphically
9 in Fig. 1. To enable a comparison of our data with Kennedy *et al.*, an equation was fitted to our
10 two-phase dataset in Table 1. For dimethyl ether an expression with three coefficients,
11
12
13
14
15
16
17
18
19
20
21

$$C_\sigma / C_0 = b_1 \tau^{-0.94} + b_2 \tau^{-0.13} + b_3 \tau^{4.3} \quad (5)$$

22 where $C_0 = 1 \text{ J} \cdot \text{mol}^{-1} \cdot \text{K}^{-1}$, $\tau = 1 - T/T_c$, $T_c = 400.378 \text{ K}$ [2], $b_1 = 2.94$, $b_2 = 83.99$, and $b_3 = 36.07$
23 was the optimal short model. We prefer the shorter three-coefficient model Eq. (5) over a
24 polynomial (5 or 6 coefficients), though the polynomial is likely to work equally well. Equation
25 (5) is valid at temperatures from (133 to 345) K along the saturated liquid curve. Percentage
26 deviations [Dev. = $100 (C_\sigma - C_{\sigma,\text{calc}})/C_\sigma$] are shown in Fig. 2. In the temperature range (133 to
27 335) K, we see that deviations are distributed randomly. At higher temperatures, $T > 335 \text{ K}$ we
28 see a deviation tail that drops to a minimum of -1.8 %, which is acceptable agreement for Eq. (5).
29 As shown in Fig. 2 in the temperature range of the Kennedy *et al.* data, (155 to 248) K, Kennedy
30 *et al.* is indistinguishable from this work. Furthermore, Fig. 2 shows that the Kennedy *et al.* data
31 deviate from Eq. (5) and from our data in Table 1 by less than the uncertainty of the Kennedy *et*
32 *al.* measurements. We conclude that this agreement is very good.
33
34
35
36
37
38
39
40
41
42
43
44
45
46
47
48
49

50 Values of the single-phase liquid heat capacity are shown in Fig. 3. The data are
51 presented on isochores, with different symbols for each filling density, in a C_v - T diagram. Most
52 liquid isochores overlap in their temperature ranges, as shown in Fig. 3. For the four highest
53
54
55
56
57
58
59
60

1
2
3 densities, C_v is observed to increase at a rate higher than the established trend. This can be
4 explained as hindered rotation of the molecules as the liquid becomes increasingly compressed,
5 resulting in a larger energy required to increase the temperature of the liquid by one kelvin. Thus,
6
7
8
9
10 for a given temperature, we observe an increasing C_v value as density increases.

11
12 When this experimental study was conducted, the only published heat capacity data for
13 dimethyl ether were the five sets of C_p data that were published from 1939 to 1991. Those values
14 were used in the development of the equation of state of Ihmels and Lemmon [1]. Since the
15 present results and those of Ref. [9] were also used by Wu *et al.*[2] their equation of state will
16 facilitate an indirect comparison with published data. Table 7 in Ref. [2] shows comparisons of
17 C_v and C_p with the equation of state of Wu *et al.* The absolute average deviation (AAD) for the
18 C_v data from this work is 0.45 % with a bias of 0.24 %. The AAD for the C_p data of Jatkar [5] is
19 7.34 % with a bias of -7.34 %. The AAD for the C_p data of Kistiakowsky and Rice [6] is 4.39 %
20 with a bias of -4.39 %. The AAD for the C_p data of Kennedy *et al.*[7] is 0.28 % with a bias of
21 -0.07 %. The AAD for the C_p data of Miyazaki *et al.*[8] is 2.50 % with a bias of -2.45 %. The
22 AAD for the C_p data of Tanaka and Higashi [9] is 6.77 % with a bias of 6.77 %. It's clear that
23 this work is in very good agreement with published heat capacities for dimethyl ether of
24 Kennedy *et al.* Conversely, the other four sources of heat capacity data show strong bias from
25 each other and are in poor agreement with the model of Ref. [2], the data of Kennedy *et al.*[7]
26 and this work.

27
28 We conducted a literature search for newer heat capacity data, which could help to
29 confirm the reliability of the model of Ref. [2] published in 2011. As mentioned earlier, the
30 present C_v data were fitted to produce the equation of state of Wu *et al.* [2], and an AAD of 0.45
31 % with a bias of 0.24 %. However, such a comparison would represent a best-case scenario, and
32
33
34
35
36
37
38
39
40
41
42
43
44
45
46
47
48
49
50
51
52
53
54
55
56
57
58
59
60

1
2
3 not an independent test of the model in Ref. [2]. When we conducted the literature search we
4
5 uncovered new C_p results by He *et al.*[10], which were published in 2014. He *et al.* reported a
6
7 relative standard uncertainty of 2.1 % for their measurements. Fortunately, He *et al.* compared
8
9 their C_p data with the model of Wu *et al.*[2] and obtained an AAD of 1.7 % with a bias of the
10
11 same amount. This allows us to conclude that the Wu *et al.*[2] model faithfully represents heat
12
13 capacity measurements within their claimed uncertainty, including reliable measurements that
14
15 were not used to develop the model.
16
17

18 19 **3.2. Derived Vapor Pressures** 20

21
22 At temperatures well below the normal boiling point, vapor pressures measured with
23
24 traditional techniques are often inaccurate. Since these conditions are under vacuum, they often
25
26 present unique experimental challenges. Among the factors that influence accuracy are (1)
27
28 inaccurate calibration (2) drift of zero point (perfect vacuum) of pressure gauges (3) difficulties
29
30 with maintaining a vacuum which increase as vacuum conditions harden and (4) as shown by
31
32 Weber [14], volatile impurities concentrate in the vapor phase as temperature and vapor pressure
33
34 decrease. Concentrating impurities are certain to influence the vapor pressure measurement,
35
36 making it appear larger than the true value for the pure substance. This situation can be remedied
37
38 to some extent, however, by extracting vapor pressure values from two-phase heat capacity
39
40 measurements. We have shown that $C_v^{(2)}$ values have excellent internal consistency and have
41
42 their lowest uncertainty below the normal boiling point because the necessary adjustments to the
43
44 $C_v^{(2)}$ measurements for vaporization and pV work are less than 0.1 % of the resulting $C_v^{(2)}$ value.
45
46
47 We elected to use this method [15] to calculate vapor pressures from the data in Table 1.
48
49
50

51
52 In the present work, only a brief summary is given for the technique to calculate vapor
53
54 pressures from isochoric internal-energy measurements in the two-phase region. A detailed
55
56
57
58
59
60

discussion is presented in the original work [15]. The method is based on the expression relating the two-phase internal energy $U^{(2)}$ to the vapor pressure,

$$(\partial U^{(2)} / \partial V)_T = T \left(\frac{dp}{dT} \right)_\sigma - p_\sigma = T^2 \left(\frac{d(p/T)}{dT} \right)_\sigma \quad (6)$$

where σ signifies a quantity evaluated on the liquid-vapor saturation boundary. By exploiting the linear dependence of $U^{(2)}$ on molar volume V , then the derivative on the left side of Eq. (6) can be replaced with a finite difference calculation,

$$(\partial U^{(2)} / \partial V^{(2)})_T = \left(\frac{U_2^{(2)} - U_1^{(2)}}{V_2^{(2)} - V_1^{(2)}} \right)_T \quad (7)$$

where, the subscripts 1 and 2 denote any two states within the two-phase region, which includes states at saturated vapor or liquid conditions. Superscript (2) denotes a bulk property, which is a thermodynamic property (H , U , V , etc.) of a sample composed of both vapor and liquid.

After calculating $(\partial U^{(2)} / \partial V^{(2)})_T$ at different temperatures between the triple point and the normal boiling point, we can fit Eq. (6) to these data using a nonlinear regression analysis [16] of the parameters in an equation for $p_\sigma(T)$. As indicated by Eq. (6), the regression analysis must fit the adjustable parameters in the difference between two equations given by $T(dp/dT)_\sigma - p_\sigma$. This is the reason why it is important to select an equation $p_\sigma = f(T)$ which is capable of fitting vapor-pressure data within their experimental uncertainty over the entire temperature range of interest. Experience has indicated which $p_\sigma(T)$ equations [17] have desirable properties.

Experimental values for $U^{(2)}$ are required to carry out the calculations with Eq. (7). We will use experimental energy-increment data from isochoric (constant $V^{(2)}$) measurements which were measured in this work. Values for $U^{(2)}$ at two or more densities are needed to calculate the change of the bulk internal energy with respect to the bulk specific volume at constant temperature. Since the calorimetric measurements provide the change of internal energy as a

function of T along a given isochore, but not the change of internal energy from one density to another, we need additional information at a reference temperature to determine the change of internal energy between two densities. This reference temperature is selected near the normal boiling point, where accurate, direct measurements of the vapor pressure are available.

The value of $(\partial U^{(2)}/\partial V^{(2)})_T$ at the reference temperature can be calculated with Eq. (6) and vapor pressure data around the reference temperature. Then, the change of internal energy from density 1 to density 2 at that reference temperature can be determined from

$$U_2^{(2)} - U_1^{(2)} = (\partial U^{(2)} / \partial V^{(2)})_T (V_2^{(2)} - V_1^{(2)}) \quad (8)$$

In this procedure, we will set the internal energy of one of the densities ($U_2^{(2)}$ or $U_1^{(2)}$) to an arbitrary value $U_i^{(2)} = 0$ at the reference temperature. Then, internal energy increments are calculated at each temperature and density based on differences in U from this reference state.

Ihmels and Lemmon [1] have shown the existence of systematic discrepancies of about $\pm 1\%$ among the two published sources of vapor pressure data for dimethyl ether in the vicinity of 182 K. One of those sources consists of a single point at 182 K. A second concern is that, at temperatures in the range ($131.66 < T/\text{K} < 172$ K), there are no published data. Our goal is to use the $U^{(2)}$ measurements in this work to calculate vapor pressures to compare with published data and to extend the range of available vapor pressures. At $p_\sigma = 101.325$ kPa, the boiling-point temperature of dimethyl ether is about 248.37 K [2] and the triple-point temperature is 131.66 K [2]. A temperature of 280 K was selected for the reference temperature due to the availability of tabulated saturation data. The internal-energy reference state, where we arbitrarily set $U^{(2)} = 0$, was selected as the saturated vapor state at 280 K. We will calculate vapor pressures for dimethyl ether from 280 K to the triple-point temperature. These calculations will give us thermodynamically consistent vapor pressures up to about 0.3 MPa which can be used to validate

1
2
3 direct measurements.

4
5 To apply Eq. (7), we need internal energies for both a high-density state and a
6 low-density state, both at the same temperature. For the low-density states, we used internal
7 energies of the saturated vapor from the Ihmels and Lemmon equation of state [1]. Each of these
8 states was paired with a high-density state from calorimetric measurements. The difference in
9 internal energy between these two curves is about 15 kJ·mol⁻¹ at the reference temperature and
10 about 20 kJ·mol⁻¹ at the triple-point temperature. The large absolute values we obtained for $\Delta U^{(2)}$
11 lead to reliable values of $(\partial U^{(2)}/\partial V^{(2)})_T$ and to accurate vapor pressures. Based on previous
12 experience [15, 17] for very long (> 200 kelvins) temperature ranges, we used an optimization
13 routine to select a functional form with four different exponents that ranged from 1 to 5 . We
14 selected a vapor pressure equation of functional form,
15
16
17
18
19
20
21
22
23
24
25
26
27

$$\ln\left(\frac{P_\sigma}{P_c}\right) = T_r^{-1} (n_1\tau + n_2\tau^{1.5} + n_3\tau^{2.5} + n_4\tau^5) \quad (9)$$

28
29 where $T_r = T/T_c$, $\tau = 1 - T/T_c$, $T_c = 400.378$ K [2], and $p_c = 5336.845$ kPa [2] for dimethyl ether.

30
31 The optimum range of Eq. (9) is $(131.66 < T/K < 280)$.

32
33 In this analysis, the change in internal energy along the high density isochore was
34 determined from two-phase calorimetric data reported in this work. We chose an isochore (approx.
35 density $\rho = 14.3$ mol·dm⁻³) that includes measurements from (133 to 300) K. For this isochore, the
36 calorimetric bomb (with a volume of approximately 78 cm³) contained 1.1453 mol of sample.
37 The energy needed to change the temperature of the sample by 1 K was fitted with the equation
38
39
40
41
42
43
44
45
46
47
48

$$Q / (n\Delta T) = a_0 + a_1 T^{-1} + a_2 T^{-2} \quad (10)$$

49
50 where Q is in J, n is in mol, and T is in K. The coefficients are: $a_0 = 1.32193502 \times 10^2$
51 J·K⁻¹·mol⁻¹, $a_1 = -1.35749740 \times 10^4$ J·mol⁻¹, and $a_2 = 9.51389556 \times 10^5$ J·K·mol⁻¹.
52
53
54
55
56
57
58
59
60

The change of internal energy along the isochore is then calculated with

$$\Delta U = \int_{T_1}^{T_2} Q / (n\Delta T) dT \quad (11)$$

where $n = 1.1453$ mol.

Although the exact bomb volume varies with temperature and pressure, we may approximate the density as a function of temperature only. The density of the *quasi-isochore* was fitted with the equation

$$\rho = b_0 + b_1 T^{-1} + b_2 T^{-2} \quad (12)$$

where ρ is in mol·dm⁻³ and the coefficients are: $b_0 = 6.06634949$ mol·dm⁻³, $b_1 = 3.83067299 \times 10^3$ mol·K·dm⁻³, and $b_2 = -2.02949652 \times 10^5$ mol·K²·dm⁻³. The molar mass used for dimethyl ether is 46.06844 g·mol⁻¹ [2]. Finally, recall that Eqs. 10 and 12 are valid for one isochore ($n = 1.1453$ mol, $\rho = 14.3$ mol·dm⁻³) in the two-phase region.

The internal energy of the saturated vapor was calculated from $U = H - PV$ with values of U calculated with the equation of state by Ihmels and Lemmon. [1] Sensitivity studies [14] have shown that the results are insensitive to the choice of a gas-phase equation of state as long as it reproduces the correct behavior of the second virial coefficients. A value of $(\partial U^{(2)} / \partial V^{(2)})_T$ at the reference temperature (280 K) was calculated with the vapor-pressure ancillary equation, Eq. (9), fitted to the published vapor pressures of Ihmels and Lemmon. [1] After application of this method to calculate vapor pressures from internal energy increments, the final vapor pressure coefficients in Eq. (9) are $n_1 = -7.1587579$, $n_2 = 2.0639544$, $n_3 = -2.31122017$, and $n_4 = -2.18605047$. Table 4 presents the vapor pressures calculated from internal energy increments in the second column, and the fourth column gives the deviation of p_σ values calculated with a global fit to available data by Wu *et al.*[2]. The Wu *et al.* model is used here to furnish an

1
2
3 independent verification of our derived vapor pressures; we observe that the Wu *et al.* model
4 deviates slightly from our vapor pressures by amounts up to 2 %, and more specifically 0.13 kPa
5 (0.52 %) at 220 K and 0.11 kPa (0.03 %) at 280 K. Figure 5 depicts deviations of published p_{σ}
6 data from Eq. (9), which is represented by the zero-line in this graph. The most rigorous test of
7 Eq. (9) is at lower temperatures ($172 < T/\text{K} < 213$) where only one experimental dataset by
8 Kennedy *et al.* [7] has been published. We observe that, in this range, the Kennedy *et al.* vapor
9 pressures deviate from Eq. 9 by less than 0.07 kPa. As mentioned above, there are no published
10 experimental p_{σ} data at temperatures between 132 K and 172 K. This indicates that the derived
11 vapor pressures in Table 4 provide useful information to thermodynamic model developers.
12
13
14
15
16
17
18
19
20
21
22

23 **3.3. Assessment of Uncertainties**

24
25
26 Uncertainty in C_v arises from several sources. Primarily, the accuracy of this method is
27 limited by the uncertainty of the temperature rise measurement and the change-of-volume work
28 adjustment. In the following discussion, the definition for the expanded uncertainty, which is
29 two times the standard uncertainty, corresponds to a coverage factor $k = 2$ and thus a
30 two-standard-deviation estimate.
31
32

33
34
35
36
37 Different sources of uncertainty, including calibration of the platinum resistance
38 thermometer, radiation to or from the thermometer head, and drift of the ice point resistance,
39 contribute to an expanded uncertainty of 0.01 K (at 100 K) to 0.03 K (at 345 K) for the absolute
40 temperature measurement. The uncertainty of the temperature rise also depends on the
41 reproducibility of temperature measurements. The temperatures assigned to the beginning (T_1)
42 and to the end (T_2) of a heating interval are determined by extrapolation of a linear temperature
43 drift (approximately $(-1 \times 10^{-3}$ to $0.5 \times 10^{-3}) \text{ K} \cdot \text{min}^{-1}$) to the midpoint time of the interval. This
44 procedure leads to an uncertainty of (0.001 to 0.004) K for the extrapolated temperatures T_1 and
45
46
47
48
49
50
51
52
53
54
55
56
57
58
59
60

1
2
3 T_2 , depending on the standard deviation of the linear function correlated. In all cases, values
4
5 from (0.002 to 0.006) K were obtained for the uncertainty of the temperature rise, $\Delta T = T_2 - T_1$.
6
7 For a typical experimental value of $\Delta T = 4$ K, this corresponds to a relative expanded uncertainty
8
9 of between (0.05 and 0.15) %.

10
11
12 The uncertainty of the change-of-volume work influences primarily the single-phase
13
14 values, since two-phase experiments are performed over a small pressure interval. The ratio of
15
16 change-of-volume work to total applied heat may be as large as 0.11 for the highest density
17
18 isochore down to 0.005 for the lowest density. Estimated uncertainties of (2.3 to 3.0) % in the
19
20 change-of-volume work are due to both the deviation of the calculated pressure derivatives and
21
22 the uncertainty of the volume change. This leads to a contribution to relative expanded
23
24 uncertainty of 0.2 % in C_v for the lowest density isochore up to 0.3 % for the highest density.
25
26

27
28 The energy applied to the calorimeter is the integral of the product of voltage and current
29
30 from the initial to the final heating time. Voltage and current are measured twenty times during a
31
32 heating interval. The measurements of the electrical quantities have a relative uncertainty of 0.01
33
34 %. However, we must account for the effect of radiation heat losses or gains which occur when
35
36 a time-dependent lag of the controller leads to a small temperature difference of about 20 mK
37
38 between the bomb and radiation shield at the beginning and end of a heating period. Since heat
39
40 transfer by radiation is proportional to $T_1^4 - T_2^4 \approx 4T^3\Delta T$, we would expect radiation losses to
41
42 substantially increase with the bomb temperature. Therefore, the relative expanded uncertainty in
43
44 the applied heat is estimated to be 0.02 % for lower temperatures and up to 0.10 % for the
45
46 highest temperatures. This leads to a contribution to relative expanded uncertainty in C_v between
47
48 (0.04 and 0.20) %.
49
50
51
52

53
54 The energy applied to the empty calorimeter has been measured in repeated experiments
55
56
57
58
59
60

1
2
3 and fitted to a function of temperature [3]; its relative uncertainty is less than 0.02 %. Its
4
5 influence on the uncertainty of the heat capacity is reduced because the ratio of the heat applied
6
7 to the empty calorimeter to the total heat varies only from 0.35 to 0.70 for the single-phase runs
8
9 and from 0.61 to 0.62 for the two-phase runs. The mass of each sample was determined with a
10
11 relative uncertainty of 0.01 % by differential weighings before and after trapping the sample. The
12
13 density calculated from this mass and the bomb volume has a relative expanded uncertainty of
14
15 approximately 0.2 %. For pressures, the uncertainty of the gauge of 7 kPa is added to the cross
16
17 term for the pressure derivative in the change-of-volume work adjustment. However, neither the
18
19 uncertainty of p nor ρ contributes appreciably to the combined uncertainty for molar heat
20
21 capacity. We may combine the various sources of experimental uncertainty using a
22
23 root-sum-of-squares formula. The relative expanded uncertainty is estimated to be 0.7 % for C_v ,
24
25 0.5 % for $C_v^{(2)}$, and 0.7 % for C_σ .

30 4. CONCLUSIONS

31
32
33 For dimethyl ether, 117 single-phase heat capacities, 90 saturated-liquid heat capacities
34
35 and 30 derived vapor pressures. Published liquid-phase heat capacity data are scarce and cover
36
37 limited ranges of temperature and pressure. Published vapor pressure data do not exist below 172
38
39 K. When considering average absolute deviations (AAD) we find agreement with published
40
41 saturated-liquid heat capacity values at constant pressure was within 0.9 %. Considering liquid
42
43 dimethyl ether, a reference quality equation of state model reproduces our experimental C_v data
44
45 with a deviation of AAD = 0.45 % (bias = 0.24 %); the same model predicts recent C_p
46
47 measurements [10] with an AAD = 1.7 %, which is within its relative expanded uncertainty of
48
49 $U_r(k=2) = 2.1$ %. By using two-phase internal energy increments and thermodynamic arguments,
50
51 we derived vapor pressures ranging from the high-vacuum region (near the triple point of 131.66
52
53
54
55
56
57
58
59
60

1
2
3 K) to several atmospheres (near 280 K). For convenience of users, we furnished both a table of
4
5 30 values and a new five-coefficient vapor pressure equation. Our derived vapor pressures
6
7 provide here-to-fore unavailable information for thermodynamic modeling, because they cover
8
9 temperatures as much as 40 °C below the lowest published measurement. Agreement of our
10
11 derived vapor pressures with published data is within 0.07 kPa at low temperatures ($172 < T/K <$
12
13 210) and is within approximately 0.5 kPa in the vicinity ($240 < T/K < 260$) of the normal boiling
14
15 point.
16
17
18

19 **ACKNOWLEDGMENTS**

20
21 We are honored to present this manuscript to this journal in memory of Dr. Kenneth
22
23 Marsh. Ken Marsh was not only a respected colleague, but also was one whose close friendship
24
25 will remain forever valued. Interestingly, Ken introduced us twelve years ago, having known
26
27 both of us separately. Ken's introduction led to a 2006 sabbatical visit by Jiangtao to Joe's lab.
28
29 The work presented here is a direct result of Jiangtao's sabbatical.
30
31
32

33 The authors are grateful to Eric Lemmon for generous technical assistance and helpful
34
35 discussions during this study. We have profitted from many discussions with Jason Widegren,
36
37 Ian Bell, and Marcia Huber.
38
39
40
41
42
43
44
45
46
47
48
49
50
51
52
53
54
55
56
57
58
59
60

Literature Cited

- (1) Ihmels, E. C.; Lemmon, E. W. Experimental Densities, Vapor Pressures, and Critical Point, and a Fundamental Equation of State for Dimethyl Ether. *Fluid Phase Equilib.* **2007**, *260*, 36-48.
- (2) Wu, J.; Zhou, Y.; Lemmon, E. W. An Equation of State for the Thermodynamic Properties of Dimethyl Ether. *J. Phys. Chem. Ref. Data* **2011**, *40*, 023104/1-16.
- (3) Goodwin, R. D. Apparatus for Determination of Pressure-Density-Temperature Relations and Specific Heats of Hydrogen to 350 Atm at Temperatures above 14 Degrees K. *J. Res. Natl. Bur. Stand. (U.S.)* **1961**, *65C*, 231-243.
- (4) Magee, J. W. Molar Heat Capacity (C_V) for Saturated and Compressed Liquid and Vapor Nitrogen from 65 to 300 K at Pressures to 30 MPa. *J. Res. Natl. Inst. Stand. Technol.* **1991**, *96*, 725-740.
- (5) Jatkar, S. K. K. Supersonic Velocity in Gases and Vapors V. Heat Capacity of Vapors of Acetone, Benzene, Cyclohexane, Hexane and Methyl, Ethyl and Propyl Ethers. *J. Indian Inst. Sci. Sec. A Sci.* **1939**, *22*, 19-37.
- (6) Kistiakowsky, G. B.; Rice, W. W. Gaseous Heat Capacities. III. *J. Chem. Phys.* **1940**, *8*, 618-622.
- (7) Kennedy R. M.; Sagenkahn, M.; Aston, J. G. The Heat Capacity and Entropy, Heats of Fusion and Vaporization, and the Vapor Pressure of Dimethyl Ether. The Density of Gaseous Dimethyl Ether. *J. Am. Chem. Soc.* **1941**, *63*, 2267-2272.
- (8) Miyazaki, M.; Kubota, H.; Tanaka, Y.; Matsuo, S. The Isobaric Specific Heat Capacities of Dimethyl Ether Under High Pressure. *12th Japan Symp. Thermophys. Prop.* **1991**, 77-80.
- (9) Tanaka, K.; Higashi, Y. Measurements of the Isobaric Specific Heat Capacity and Density

- 1
2
3 for Dimethyl Ether in the Liquid State. *J. Chem. Eng. Data* **2010**, *55*, 2658-2661.
4
5
6 (10) He, Y.; Gao, N.; Jiang, Y.; Ren, B.; Chen, G. Isobaric Heat Capacity Measurements for
7
8 Dimethyl Ether and 1,1-Difluoroethane in the Liquid Phase at Temperatures from 305 K
9
10 to 365 K and Pressures up to 5 MPa. *J. Chem. Eng. Data* **2014**, *59*, 2885-2890.
11
12 (11) Goodwin, R. D.; Weber, L. A. Specific Heats C_V of Fluid Oxygen from the Triple Point
13
14 to 300 K at Pressures to 350 Atmospheres. *J. Res. Natl. Bur. Stand. (U.S.)* **1969**, *73A*,
15
16 15-24.
17
18 (12) Jacobsen, R. T; Stewart, R. B. Thermodynamic Properties of Nitrogen Including Liquid
19
20 and Vapor Phases from 63 K to 2000 K with Pressures to 10,000 Bar. *J. Phys. Chem. Ref.*
21
22 *Data* **1973**, *2*, 757-922.
23
24
25 (13) Rowlinson, J. S. *Liquids and Liquid Mixtures*; Butterworths: London, **1969**, p. 37.
26
27 (14) Weber, L. A. Criteria for Establishing Accurate Vapor-Pressure Curves. *Int. J. Refrig.*
28
29 **1994**, *17*, 117-122.
30
31
32 (15) Duarte-Garza. H. A.; Magee, J. W. Subatmospheric Vapor Pressures Evaluated from
33
34 Internal-Energy Measurements. *Int. J. Thermophys.* **1997**, *18*, 173-193.
35
36
37 (16) Boggs, P. T.; Byrd, R. H.; Rogers, J. E.; Schnabel, R. B. NISTIR 4834, *User's Reference*
38
39 *Guide for ODRPACK Version 2.01, Software for Weighted Orthogonal Distance*
40
41 *Regression*; NIST: Gaithersburg, MD, **1992**.
42
43
44 (17) Duarte-Garza. H. A.; Magee, J. W. Subatmospheric Vapor Pressures for Fluoromethane
45
46 (R41), 1,1-Difluoroethane (R152a), and 1,1,1-Trifluoroethane (R143a) Evaluated from
47
48 Internal-Energy Measurements. *Int. J. Thermophys.* **1999**, *19*, 1467-1481.
49
50
51 (18) Wu, J. T.; Yin, J. G. Vapor Pressure Measurements of Dimethyl Ether from (213 to 393)
52
53
54 K. *J. Chem. Eng. Data* **2008**, *53*, 2247-2249.
55
56
57
58
59
60

- 1
2
3 (19) Corvaro, F.; Nicola, G. D.; Polonara, F.; Santori, G. Saturated Pressure Measurements of
4 Dimethyl Ether at Temperatures from (219 to 361) K. *J. Chem. Eng. Data* **2006**, *51*,
5 1469-1472.
6
7
8
9
10 (20) Valtz, A.; Gicquel, L.; Coquelet, C.; Richon, D. Vapour-liquid equilibrium data for the
11 1,1,1,2 tetrafluoroethane (R134a) + dimethyl ether (DME) system at temperatures from
12 293.18 to 358.15 K and pressures up to about 3 MPa. *Fluid Phase Equilib.* **2005**, *230*,
13 184-191.
14
15
16
17
18 (21) Fedele, L.; Bobbo, S.; Stefani, V. D.; Camporese, R.; Stryjek, R. Isothermal VLE
19 Measurements for Difluoromethane + Dimethyl Ether and an Evaluation of Hydrogen
20 Bonding. *J. Chem. Eng. Data* **2005**, *50*, 128-132.
21
22
23
24
25 (22) Bobbo, S.; Fedele, L.; Camporese, R.; Stryjek, R. Hydrogen-bonding of HFCs with
26 dimethyl ether: evaluation by isothermal VLE measurements. *Fluid Phase Equilib.* **2002**, *199*,
27 153-160.
28
29
30
31
32 (23) Daiguji, H.; Hihara, E. Vapor-Liquid Equilibrium for Dimethyl Ether + Propyl Acetate. *J.*
33 *Chem. Eng. Data* **2003**, *48*, 266-271.
34
35
36
37
38
39
40
41
42
43
44
45
46
47
48
49
50
51
52
53
54
55
56
57
58
59
60

List of Tables

Table 1. Two-phase heat capacity $C_v^{(2)}$ and heat capacity of saturated liquid C_σ of dimethyl ether.

Table 2. Heat capacity C_v of compressed liquid dimethyl ether.

Table 3. Densities of liquid dimethyl ether.

Table 4. Vapor pressures of dimethyl ether derived from $U^{(2)}$ measurements.

List of Figures

Figure 1. Experimental saturated-liquid heat capacity $C_\sigma/\text{J}\cdot\text{mol}^{-1}\cdot\text{K}^{-1}$ values for dimethyl ether:

☆ This work; ○ Kennedy *et al.* [7].

Figure 2. Comparison of experimental C_σ results [Dev. = $100 (C_\sigma - C_{\sigma,\text{calc}})/C_\sigma$] for dimethyl ether; $C_{\sigma,\text{calc}}$ values calculated with Eq. (5): ☆ This work; ○ Kennedy *et al.* [7].

Figure 3. Experimental compressed liquid heat capacity $C_v/\text{J}\cdot\text{mol}^{-1}\cdot\text{K}^{-1}$ data for dimethyl ether:

■ $18.5 \text{ mol}\cdot\text{dm}^{-3}$; ● $18.0 \text{ mol}\cdot\text{dm}^{-3}$; ▲ $17.3 \text{ mol}\cdot\text{dm}^{-3}$; ▼ $16.7 \text{ mol}\cdot\text{dm}^{-3}$; ◆ $16.1 \text{ mol}\cdot\text{dm}^{-3}$; ◀ $15.6 \text{ mol}\cdot\text{dm}^{-3}$; ▶ $15.0 \text{ mol}\cdot\text{dm}^{-3}$; ◆ $14.3 \text{ mol}\cdot\text{dm}^{-3}$; ★ $13.6 \text{ mol}\cdot\text{dm}^{-3}$.

Figure 4. Comparison of experimental C_v results [Dev. = $100 (C_v - C_{v,\text{calc}})/C_v$] for dimethyl ether; $C_{v,\text{calc}}$ values calculated with the model of Ihmels and Lemmon [1] : □ $18.5 \text{ mol}\cdot\text{dm}^{-3}$; ○ $18.0 \text{ mol}\cdot\text{dm}^{-3}$; ▲ $17.3 \text{ mol}\cdot\text{dm}^{-3}$; ▼ $16.7 \text{ mol}\cdot\text{dm}^{-3}$; ◆ $16.1 \text{ mol}\cdot\text{dm}^{-3}$; ◀ $15.6 \text{ mol}\cdot\text{dm}^{-3}$; ▶ $15.0 \text{ mol}\cdot\text{dm}^{-3}$; * $14.3 \text{ mol}\cdot\text{dm}^{-3}$; ☆ $13.6 \text{ mol}\cdot\text{dm}^{-3}$.

Figure 5. Comparison of published vapor pressures [Dev. = $p_\sigma - p_{\sigma,\text{cal}}$] with values calculated with Eq. (9) - this work, derived from experimental $U^{(2)}$ increments: ▲, Wu and Yin [18]; ■, Corvaro *et al.* [19]; ◀, Ihmels and Lemmon [1]; ▶, Valtz *et al.* [20]; ☆, Kennedy *et al.* [7]; ◆, Fedele *et al.* [21]; *, Bobbo *et al.* [22]; +, Daiguji and Hihara [23]; —, Wu and Yin [18]; ----, Ihmels and Lemmon [1].

Table 1. Two-phase heat capacity $C_V^{(2)}$ and heat capacity of saturated liquid C_σ of dimethyl ether.

T/K	$\rho_\sigma^a/\text{mol}\cdot\text{dm}^{-3}$	P_σ^a/MPa	$C_V^{(2)b}/\text{J}\cdot\text{mol}^{-1}\cdot\text{K}^{-1}$	$C_\sigma/\text{J}\cdot\text{mol}^{-1}\cdot\text{K}^{-1}$	Dev. ^c /%
133.47	19.100	<1.0E-4	99.41	99.41	0.26
136.11	19.031	<1.0E-4	98.99	98.99	-0.05
138.75	18.963	<1.0E-4	99.09	99.09	0.15
141.37	18.895	<1.0E-4	98.75	98.75	-0.11
143.97	18.827	<1.0E-4	98.65	98.64	-0.14
146.56	18.759	<1.0E-4	98.99	98.99	0.28
149.14	18.691	<1.0E-4	99.24	99.23	0.58
151.70	18.624	1.0E-4	99.00	98.99	0.39
154.26	18.557	1.0E-4	98.78	98.77	0.20
156.80	18.490	1.0E-4	98.65	98.65	0.10
159.33	18.423	2.0E-4	98.45	98.43	-0.09
161.84	18.357	2.0E-4	98.69	98.67	0.16
164.35	18.290	3.0E-4	98.62	98.60	0.09
166.84	18.224	4.0E-4	98.48	98.46	-0.06
169.32	18.158	5.0E-4	98.35	98.32	-0.21
171.79	18.093	6.0E-4	98.42	98.39	-0.17
174.26	18.027	8.0E-4	98.47	98.44	-0.16
176.71	17.962	1.0E-3	98.51	98.47	-0.16
179.15	17.896	1.20E-3	98.78	98.73	0.05
181.58	17.831	1.50E-3	98.84	98.78	0.06
184.00	17.766	1.90E-3	98.61	98.54	-0.25
186.41	17.701	2.40E-3	98.88	98.80	-0.06
188.82	17.636	2.90E-3	99.07	98.98	0.05
191.21	17.572	3.50E-3	99.01	98.90	-0.11
193.60	17.507	4.20E-3	99.23	99.11	0.01
195.98	17.442	5.00E-3	99.13	98.99	-0.21
198.36	17.377	6.00E-3	99.17	99.02	-0.28
200.73	17.313	7.10E-3	99.27	99.09	-0.32
203.08	17.248	8.40E-3	99.27	99.08	-0.45
205.44	17.183	9.90E-3	99.53	99.32	-0.33
207.79	17.119	0.012	100.13	99.89	0.12
210.13	17.054	0.014	100.41	100.15	0.24
212.46	16.989	0.016	100.25	99.96	-0.09
214.79	16.924	0.018	100.46	100.15	-0.05
217.12	16.859	0.021	100.60	100.26	-0.09
219.43	16.794	0.024	100.45	100.09	-0.42
221.74	16.729	0.027	100.51	100.12	-0.56
224.04	16.664	0.031	100.63	100.21	-0.64
226.34	16.599	0.035	101.10	100.65	-0.38
228.64	16.533	0.040	101.58	101.10	-0.12

1
2
3
4
5
6
7
8
9
10
11
12
13
14
15
16
17
18
19
20
21
22
23
24
25
26
27
28
29
30
31
32
33
34
35
36
37
38
39
40
41
42
43
44
45
46
47
48
49
50
51
52
53
54
55
56
57
58
59
60

230.92	16.468	0.045	101.60	101.10	-0.31
233.21	16.402	0.050	101.94	101.41	-0.20
235.49	16.336	0.056	102.32	101.75	-0.07
237.76	16.270	0.063	102.28	101.68	-0.35
240.03	16.204	0.070	102.56	101.94	-0.31
242.31	16.137	0.077	102.80	102.15	-0.33
244.57	16.071	0.086	103.28	102.60	-0.11
246.84	16.003	0.095	103.19	102.48	-0.47
249.11	15.936	0.105	104.03	103.29	0.08
251.38	15.868	0.115	103.57	102.81	-0.64
253.64	15.800	0.127	103.78	103.00	-0.71
255.90	15.731	0.139	104.25	103.44	-0.54
258.16	15.663	0.152	104.64	103.81	-0.46
260.42	15.593	0.167	104.93	104.08	-0.48
262.68	15.524	0.182	105.61	104.75	-0.12
264.94	15.453	0.198	106.39	105.51	0.31
267.20	15.383	0.215	106.80	105.91	0.38
269.47	15.312	0.234	107.32	106.42	0.55
271.72	15.240	0.254	107.05	106.14	-0.02
273.98	15.168	0.275	107.17	106.27	-0.24
276.24	15.095	0.297	108.02	107.11	0.22
278.50	15.022	0.320	108.89	108.00	0.70
280.77	14.948	0.345	108.96	108.08	0.42
283.02	14.874	0.372	109.22	108.35	0.30
285.29	14.799	0.400	109.74	108.89	0.43
287.55	14.723	0.429	110.24	109.42	0.53
289.82	14.646	0.460	110.25	109.46	0.16
292.08	14.569	0.493	110.74	110.00	0.24
294.36	14.491	0.528	111.42	110.71	0.47
296.63	14.412	0.564	111.15	110.49	-0.17
298.90	14.332	0.603	111.97	111.38	0.18
301.19	14.251	0.643	112.10	111.57	-0.11
303.45	14.170	0.685	112.80	112.35	0.10
305.74	14.087	0.730	113.10	112.73	-0.06
308.02	14.004	0.776	113.77	113.50	0.11
310.30	13.919	0.825	115.06	114.89	0.80
312.58	13.833	0.876	115.66	115.60	0.86
314.87	13.747	0.929	116.06	116.12	0.75
317.16	13.658	0.985	115.92	116.12	0.16
319.44	13.569	1.043	117.28	117.62	0.83
323.96	13.389	1.166	118.42	119.09	0.79
326.26	13.296	1.232	119.18	120.03	0.89
328.57	13.200	1.301	119.45	120.51	0.57
330.88	13.103	1.373	120.16	121.43	0.58
333.20	13.004	1.449	120.45	121.96	0.22
335.54	12.902	1.528	121.01	122.78	0.06

3	337.89	12.798	1.610	120.75	122.80	-0.81
4	340.24	12.692	1.696	121.73	124.08	-0.69
5	342.62	12.582	1.787	122.22	124.90	-1.03
6	345.00	12.469	1.881	122.15	125.19	-1.85

^a Saturated liquid properties calculated with the model of Ihmels and Lemmon [1].

^b Standard uncertainties are $u(T) = 0.02$ K; relative expanded ($k = 2$) uncertainties are $U_r(C_V^{(2)}) = 0.5\%$,

$U_r(C_\sigma) = 0.7\%$

^c Dev. = $100 (C_\sigma - C_{\sigma,\text{calc}})/C_\sigma$; $C_{\sigma,\text{calc}}$ values calculated with Eq 5.

Table 2. Heat capacity C_v of compressed liquid dimethyl ether.

T /K	ρ /mol·dm ⁻³	P /MPa	C_v^a /J·K ⁻¹ ·mol ⁻¹	Dev. ^b /%
157.53	18.509	4.013	69.69	-2.24
159.72	18.498	8.322	69.60	-1.83
161.90	18.487	12.544	69.78	-1.10
164.07	18.476	16.672	69.67	-0.86
166.23	18.465	20.708	69.85	-0.25
168.38	18.455	24.704	69.65	-0.24
170.51	18.444	28.650	69.79	0.21
172.64	18.434	32.529	70.05	0.79
176.39	18.007	3.776	68.85	-1.37
178.57	17.997	7.593	68.76	-1.15
180.74	17.987	11.350	68.76	-0.85
182.90	17.977	15.062	68.62	-0.80
185.05	17.968	18.718	68.78	-0.35
187.20	17.958	22.325	68.84	-0.08
189.34	17.948	25.885	68.95	0.23
191.46	17.939	29.382	69.00	0.43
193.58	17.929	32.823	69.21	0.83
200.60	17.351	3.313	68.02	-1.00
202.77	17.343	6.569	67.99	-0.85
204.93	17.334	9.792	67.70	-1.13
207.08	17.325	12.969	68.02	-0.53
209.23	17.316	16.115	68.00	-0.46
211.37	17.308	19.219	68.42	0.23
213.50	17.299	22.288	68.53	0.44
215.62	17.291	25.311	68.58	0.55
217.74	17.282	28.297	69.12	1.33
219.85	17.274	31.246	69.00	1.16
223.34	16.721	2.896	67.94	-0.59
225.51	16.713	5.714	67.91	-0.55
227.67	16.706	8.494	68.08	-0.25
229.82	16.698	11.254	68.44	0.32
231.97	16.690	13.976	68.41	0.28
234.11	16.683	16.676	68.64	0.61
236.24	16.675	19.342	68.90	0.96
238.36	16.668	21.979	68.71	0.64
240.48	16.660	24.585	68.77	0.67
242.59	16.653	27.158	69.15	1.15
244.69	16.645	29.702	69.45	1.49
246.78	16.638	32.213	69.76	1.84
245.08	16.099	2.602	68.32	-0.34
247.24	16.092	5.030	68.61	0.09
249.40	16.085	7.443	68.82	0.38

3	251.55	16.078	9.828	69.15	0.82
4	253.70	16.072	12.195	69.10	0.69
5	255.84	16.065	14.539	69.14	0.68
6	257.97	16.058	16.865	69.11	0.56
7	260.09	16.051	19.157	69.43	0.92
8	262.21	16.045	21.436	69.63	1.10
9	264.32	16.038	23.690	69.84	1.27
10	266.43	16.032	25.920	69.92	1.25
11	268.52	16.025	28.128	69.96	1.17
12	270.62	16.019	30.316	69.95	1.00
13	272.69	16.012	32.476	70.70	1.90
14	261.13	15.623	2.479	69.34	0.45
15	263.30	15.617	4.661	69.49	0.62
16	265.47	15.611	6.829	69.28	0.26
17	267.63	15.604	8.973	69.82	0.96
18	269.79	15.598	11.103	69.61	0.57
19	271.93	15.592	13.210	69.63	0.50
20	274.07	15.586	15.304	70.14	1.10
21	276.21	15.580	17.379	70.25	1.13
22	278.33	15.574	19.435	70.27	1.02
23	280.45	15.568	21.472	70.38	1.02
24	282.56	15.562	23.487	70.94	1.64
25	284.67	15.556	25.491	70.96	1.50
26	286.77	15.550	27.476	70.72	0.99
27	288.86	15.544	29.439	71.64	2.08
28	290.95	15.538	31.396	71.89	2.23
29	293.04	15.532	33.333	71.85	1.97
30	279.17	15.069	2.674	69.72	-0.20
31	281.36	15.063	4.596	69.98	0.09
32	283.54	15.057	6.506	69.97	-0.02
33	285.71	15.052	8.399	70.42	0.50
34	287.87	15.046	10.279	70.77	0.87
35	290.03	15.041	12.145	71.02	1.08
36	292.18	15.035	14.000	71.24	1.24
37	294.33	15.030	15.843	71.24	1.08
38	296.47	15.024	17.674	70.96	0.52
39	298.61	15.019	19.489	71.48	1.07
40	300.75	15.013	21.296	71.95	1.53
41	302.88	15.008	23.091	71.44	0.63
42	305.01	15.003	24.872	71.85	0.99
43	307.14	14.997	26.644	72.77	2.04
44	309.27	14.992	28.409	73.16	2.34
45	311.39	14.986	30.163	72.97	1.87
46	313.52	14.981	31.911	73.20	1.95
47	315.65	14.976	33.651	73.00	1.44
48	300.73	14.349	2.646	71.27	0.00

1
2
3
4
5
6
7
8
9
10
11
12
13
14
15
16
17
18
19
20
21
22
23
24
25
26
27
28
29
30
31
32
33
34
35
36
37
38
39
40
41
42
43
44
45
46
47
48
49
50
51
52
53
54
55
56
57
58
59
60

302.96	14.345	4.292	71.08	-0.38
305.18	14.340	5.930	71.96	0.72
307.41	14.335	7.569	72.11	0.78
309.62	14.330	9.196	71.88	0.31
311.84	14.325	10.814	72.56	1.08
314.06	14.320	12.436	72.39	0.67
316.28	14.315	14.048	72.58	0.75
318.50	14.310	15.656	72.87	0.95
320.74	14.305	17.265	73.03	0.96
322.97	14.300	18.872	73.22	1.00
325.22	14.295	20.482	73.26	0.83
327.49	14.291	22.098	73.84	1.37
329.78	14.285	23.723	73.46	0.62
332.09	14.280	25.355	73.79	0.81
334.44	14.275	27.002	74.11	0.97
336.81	14.270	28.665	74.55	1.28
339.21	14.265	30.343	75.43	2.15
341.66	14.259	32.044	75.07	1.39
344.14	14.254	33.761	74.99	0.98
320.54	13.613	2.597	72.71	-0.34
323.02	13.609	4.128	72.98	-0.11
325.50	13.604	5.662	73.54	0.50
328.01	13.599	7.206	73.45	0.20
330.53	13.595	8.756	73.25	-0.26
333.07	13.590	10.311	73.52	-0.10
335.63	13.585	11.877	73.69	-0.08
338.21	13.580	13.448	74.18	0.35
340.82	13.575	15.034	74.59	0.65
343.45	13.570	16.629	74.42	0.16

^a Standard uncertainty is $u(T) = 0.02$ K; expanded ($k = 2$) uncertainty is $U_c(p) = 0.035$ MPa; relative expanded ($k = 2$) uncertainties are $U_r(\rho) = 0.2$ %, $U_r(C_v) = 0.7$ %.

^b Dev. = $100 (C_v - C_{v,calc})/C_v$; $C_{v,calc}$ values calculated with the model of Ihmels and Lemmon [1].

Table 3. Densities of liquid dimethyl ether.

T	p	$\rho_{\text{exp}}^{\text{a}}$	$\rho_{\text{calc}}^{\text{b}}$	Dev. ^c
K	MPa	mol·dm ⁻³		%
157.53	4.013	18.509	18.518	-0.05
159.72	8.322	18.498	18.511	-0.07
161.90	12.544	18.487	18.503	-0.09
164.07	16.672	18.476	18.494	-0.10
166.23	20.708	18.465	18.484	-0.10
168.38	24.704	18.455	18.475	-0.11
170.51	28.650	18.444	18.465	-0.11
172.64	32.529	18.434	18.455	-0.11
176.39	3.776	18.007	18.021	-0.08
178.57	7.593	17.997	18.014	-0.09
180.74	11.350	17.987	18.007	-0.11
182.90	15.062	17.977	17.999	-0.12
185.05	18.718	17.968	17.991	-0.13
187.20	22.325	17.958	17.982	-0.13
189.34	25.885	17.948	17.974	-0.14
191.46	29.382	17.939	17.965	-0.14
193.58	32.823	17.929	17.956	-0.15
200.60	3.313	17.351	17.370	-0.11
202.77	6.569	17.343	17.364	-0.12
204.93	9.792	17.334	17.357	-0.13
207.08	12.969	17.325	17.350	-0.14
209.23	16.115	17.316	17.343	-0.16
211.37	19.219	17.308	17.336	-0.16
213.50	22.288	17.299	17.328	-0.17
215.62	25.311	17.291	17.320	-0.17
217.74	28.297	17.282	17.312	-0.17
219.85	31.246	17.274	17.304	-0.17
223.34	2.896	16.721	16.741	-0.12
225.51	5.714	16.713	16.735	-0.13
227.67	8.494	16.706	16.729	-0.14
229.82	11.254	16.698	16.723	-0.15
231.97	13.976	16.690	16.717	-0.16
234.11	16.676	16.683	16.710	-0.16
236.24	19.342	16.675	16.704	-0.17
238.36	21.979	16.668	16.697	-0.17
240.48	24.585	16.660	16.690	-0.18
242.59	27.158	16.653	16.682	-0.17
244.69	29.702	16.645	16.675	-0.18
246.78	32.213	16.638	16.668	-0.18
245.08	2.602	16.099	16.117	-0.11

1
2
3
4
5
6
7
8
9
10
11
12
13
14
15
16
17
18
19
20
21
22
23
24
25
26
27
28
29
30
31
32
33
34
35
36
37
38
39
40
41
42
43
44
45
46
47
48
49
50
51
52
53
54
55
56
57
58
59
60

247.24	5.030	16.092	16.112	-0.12
249.40	7.443	16.085	16.107	-0.14
251.55	9.828	16.078	16.102	-0.15
253.70	12.195	16.072	16.096	-0.15
255.84	14.539	16.065	16.090	-0.16
257.97	16.865	16.058	16.084	-0.16
260.09	19.157	16.051	16.078	-0.17
262.21	21.436	16.045	16.072	-0.17
264.33	23.690	16.038	16.066	-0.17
266.43	25.920	16.032	16.059	-0.17
268.52	28.128	16.025	16.053	-0.17
270.62	30.316	16.019	16.046	-0.17
272.69	32.476	16.012	16.039	-0.17
261.13	2.479	15.623	15.638	-0.10
263.30	4.661	15.617	15.634	-0.11
265.47	6.829	15.611	15.629	-0.12
267.63	8.973	15.604	15.624	-0.13
269.79	11.103	15.598	15.619	-0.13
271.93	13.210	15.592	15.614	-0.14
274.07	15.304	15.586	15.609	-0.15
276.21	17.379	15.580	15.603	-0.15
278.33	19.435	15.574	15.597	-0.15
280.45	21.472	15.568	15.592	-0.15
282.56	23.487	15.562	15.586	-0.15
284.67	25.491	15.556	15.580	-0.15
286.77	27.476	15.550	15.573	-0.15
288.86	29.439	15.544	15.567	-0.15
290.95	31.396	15.538	15.561	-0.15
293.04	33.333	15.532	15.555	-0.15
279.17	2.674	15.069	15.083	-0.09
281.36	4.596	15.063	15.079	-0.11
283.54	6.506	15.057	15.075	-0.12
285.71	8.399	15.052	15.071	-0.13
287.87	10.279	15.046	15.066	-0.13
290.03	12.145	15.041	15.061	-0.13
292.18	14.000	15.035	15.057	-0.15
294.33	15.843	15.030	15.052	-0.15
296.47	17.674	15.024	15.047	-0.15
298.61	19.489	15.019	15.041	-0.15
300.75	21.296	15.013	15.036	-0.15
302.88	23.091	15.008	15.030	-0.15
305.01	24.872	15.003	15.025	-0.15
307.14	26.644	14.997	15.019	-0.15
309.27	28.409	14.992	15.013	-0.14
311.39	30.163	14.986	15.008	-0.15

3	313.52	31.911	14.981	15.002	-0.14
4	315.65	33.651	14.976	14.996	-0.13
5	300.73	2.646	14.349	14.361	-0.08
6	302.96	4.292	14.345	14.358	-0.09
7	305.18	5.930	14.340	14.355	-0.10
8	307.41	7.569	14.335	14.351	-0.11
9	309.62	9.196	14.330	14.347	-0.12
10	311.84	10.814	14.325	14.343	-0.13
11	314.06	12.436	14.320	14.338	-0.13
12	316.28	14.048	14.315	14.334	-0.13
13	318.50	15.656	14.310	14.329	-0.13
14	320.74	17.265	14.305	14.324	-0.13
15	322.97	18.872	14.300	14.320	-0.14
16	325.22	20.482	14.295	14.314	-0.13
17	327.49	22.098	14.291	14.309	-0.13
18	329.78	23.723	14.285	14.304	-0.13
19	332.09	25.355	14.280	14.298	-0.13
20	334.44	27.002	14.275	14.293	-0.13
21	336.81	28.665	14.270	14.287	-0.12
22	339.21	30.343	14.265	14.281	-0.11
23	341.66	32.044	14.259	14.275	-0.11
24	344.14	33.761	14.254	14.268	-0.10
25	320.54	2.597	13.613	13.624	-0.08
26	323.02	4.128	13.609	13.621	-0.09
27	325.50	5.662	13.604	13.618	-0.10
28	328.01	7.206	13.599	13.614	-0.11
29	330.53	8.756	13.595	13.610	-0.11
30	333.07	10.311	13.590	13.606	-0.12
31	335.63	11.877	13.585	13.602	-0.13
32	338.21	13.448	13.580	13.597	-0.13
33	340.82	15.034	13.575	13.592	-0.13
34	343.45	16.629	13.570	13.587	-0.13

^a Standard uncertainty is $u(T) = 0.02$ K; expanded ($k = 2$) uncertainty is $u(p) = 0.035$ MPa; relative expanded ($k = 2$) uncertainty is $U_r(\rho) = 0.2$ %.

^b Density calculated with model of Ihmels and Lemmon [1].

^c Density Dev. = $100 (\rho_{\text{exp}} - \rho_{\text{calc}})/\rho_{\text{exp}}$; ρ_{calc} values calculated with model of Ihmels and Lemmon [1].

Table 4. Vapor pressures of dimethyl ether derived from $U^{(2)}$ measurements.

T	$p_{\sigma, \text{this work.}}^a$	$p_{\sigma, \text{calc}}^b$	Dev. ^c
K	(kPa)		(kPa)
135.00	0.004	0.004	0.000
140.00	0.010	0.010	0.000
145.00	0.022	0.021	0.001
150.00	0.045	0.044	0.001
155.00	0.088	0.086	0.002
160.00	0.163	0.160	0.003
165.00	0.292	0.287	0.005
170.00	0.502	0.494	0.008
175.00	0.833	0.821	0.012
180.00	1.338	1.321	0.017
185.00	2.087	2.063	0.024
190.00	3.168	3.135	0.033
195.00	4.692	4.648	0.044
200.00	6.792	6.736	0.056
205.00	9.629	9.557	0.072
210.00	13.389	13.301	0.088
215.00	18.291	18.184	0.107
220.00	24.579	24.453	0.126
225.00	32.531	32.383	0.148
230.00	42.452	42.283	0.169
235.00	54.677	54.489	0.188
240.00	69.572	69.365	0.207
245.00	87.528	87.305	0.223
250.00	108.961	108.728	0.233
255.00	134.316	134.077	0.239
260.00	164.056	163.819	0.237
265.00	198.668	198.442	0.226
270.00	238.658	238.456	0.202
275.00	284.551	284.385	0.166
280.00	336.886	336.775	0.111

^a This work derived with Eqs (6), (7) and (8) and measured internal energy $U^{(2)}$ increments; standard uncertainty is $u(T) = 0.02$ K; relative standard uncertainty is $u_r(p_{\sigma}) = 0.6\%$;

^b Calculated with model of Wu *et al.* [2].

^c Dev. = $p_{\sigma, \text{this work}} - p_{\sigma, \text{calc}}$; $p_{\sigma, \text{calc}}$ values calculated with model of Wu *et al.* [2].

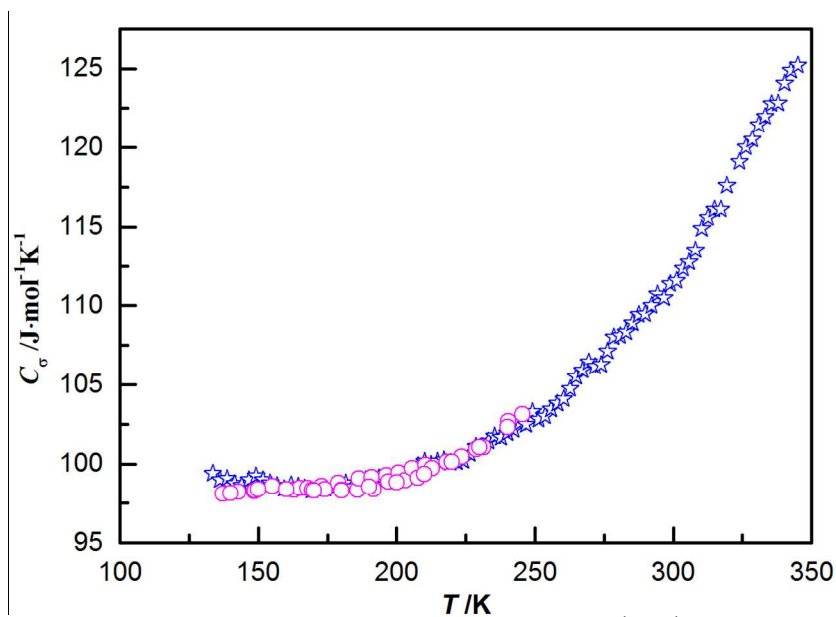


Figure 1. Experimental saturated-liquid heat capacity $C_{\sigma}/\text{J}\cdot\text{mol}^{-1}\cdot\text{K}^{-1}$ values for dimethyl ether:

☆ This work; ○ Kennedy *et al.* [7].

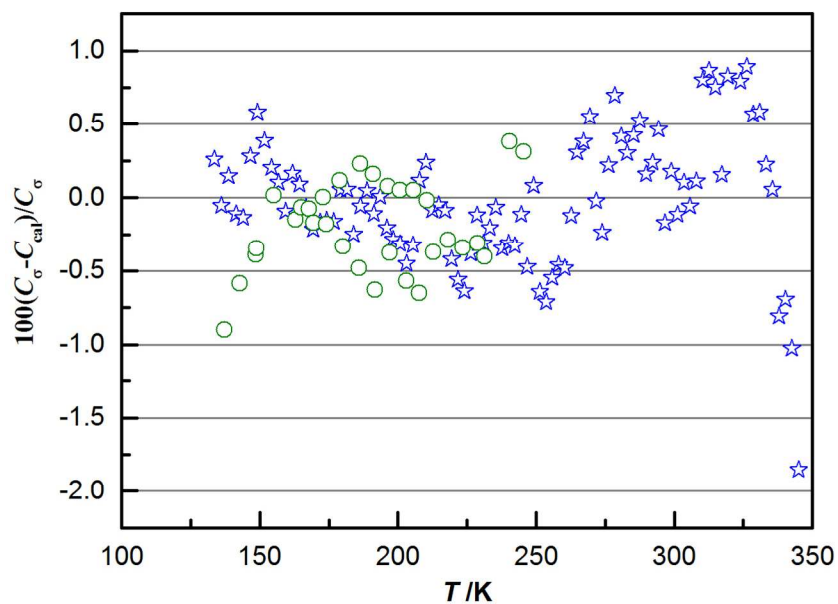


Figure 2. Comparison of experimental C_{σ} results [Dev. = $100(C_{\sigma} - C_{\sigma,\text{calc}})/C_{\sigma}$] for dimethyl ether; $C_{\sigma,\text{calc}}$ values calculated with Eq. (5): ☆ This work; ○ Kennedy *et al.* [7].

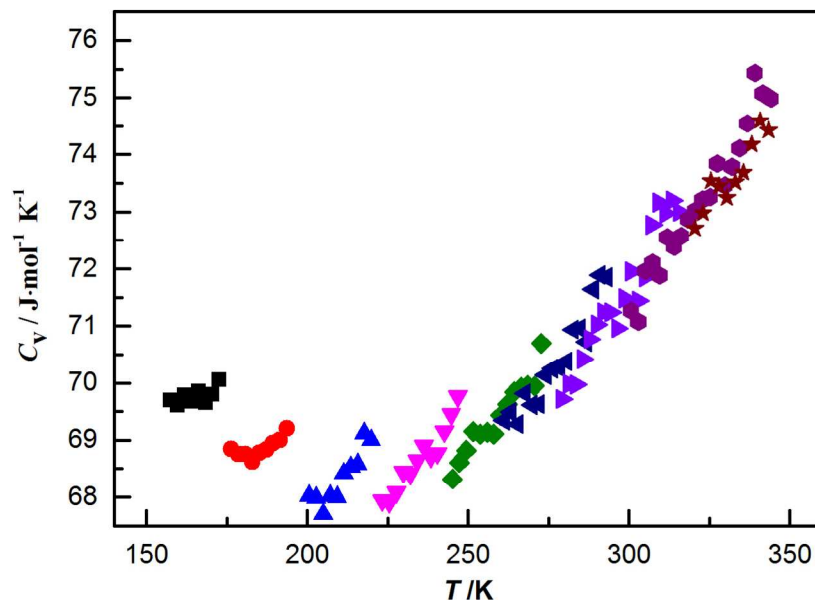


Figure 3. Experimental compressed liquid heat capacity $C_v/\text{J}\cdot\text{mol}^{-1}\cdot\text{K}^{-1}$ data for dimethyl ether: \blacksquare $18.5\text{ mol}\cdot\text{dm}^{-3}$; \bullet $18.0\text{ mol}\cdot\text{dm}^{-3}$; \blacktriangle $17.3\text{ mol}\cdot\text{dm}^{-3}$; \blacktriangledown $16.7\text{ mol}\cdot\text{dm}^{-3}$; \blacklozenge $16.1\text{ mol}\cdot\text{dm}^{-3}$; \blacktriangleleft $15.6\text{ mol}\cdot\text{dm}^{-3}$; \blacktriangleright $15.0\text{ mol}\cdot\text{dm}^{-3}$; \blacklozenge $14.3\text{ mol}\cdot\text{dm}^{-3}$; \star $13.6\text{ mol}\cdot\text{dm}^{-3}$.

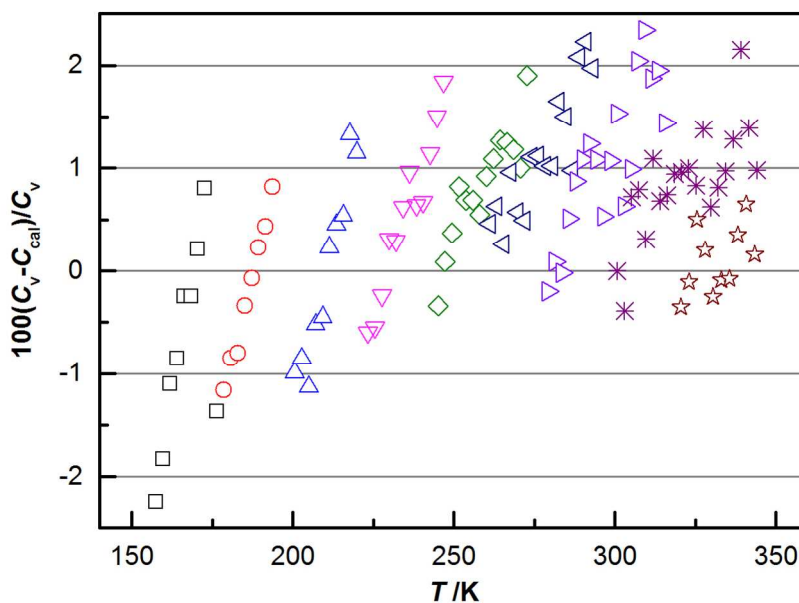


Figure 4. Comparison of experimental C_v results [Dev. = $100 (C_v - C_{v,\text{calc}})/C_v$] for dimethyl ether; $C_{v,\text{calc}}$ values calculated with the model of Ihmels and Lemmon [1]: \square $18.5\text{ mol}\cdot\text{dm}^{-3}$; \circ $18.0\text{ mol}\cdot\text{dm}^{-3}$; \triangle $17.3\text{ mol}\cdot\text{dm}^{-3}$; \triangledown $16.7\text{ mol}\cdot\text{dm}^{-3}$; \lozenge $16.1\text{ mol}\cdot\text{dm}^{-3}$; \triangleleft $15.6\text{ mol}\cdot\text{dm}^{-3}$; \triangleright $15.0\text{ mol}\cdot\text{dm}^{-3}$; \lozenge $14.3\text{ mol}\cdot\text{dm}^{-3}$; \star $13.6\text{ mol}\cdot\text{dm}^{-3}$.

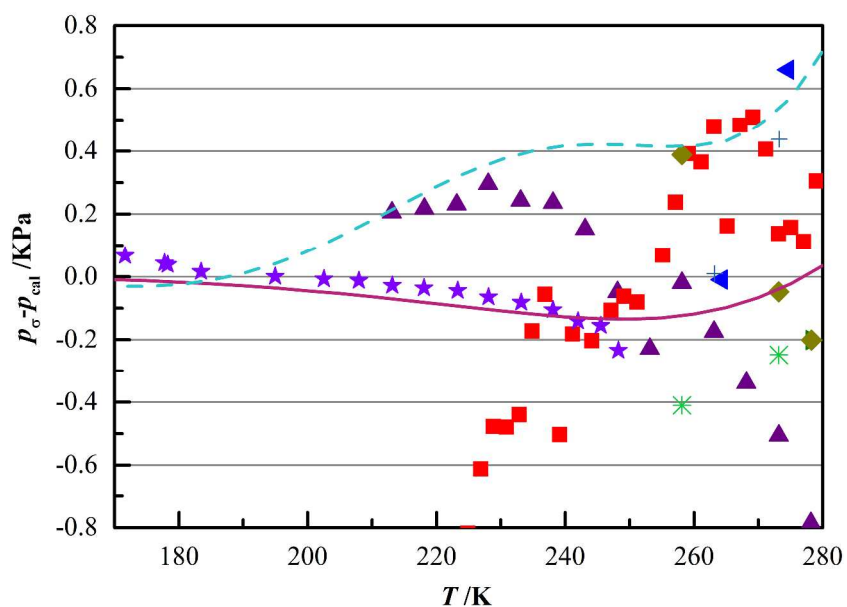


Figure 5. Comparison of published vapor pressures [$\text{Dev.} = p_{\sigma} - p_{\sigma,\text{cal}}$] with values calculated with Eq. (9) - this work, derived from experimental $U^{(2)}$ increments: \blacktriangle , Wu and Yin [18]; \blacksquare , Corvaro *et al.* [19]; \blacktriangleleft , Ihmels and Lemmon [1]; \blacktriangleright , Valtz *et al.* [20]; \star , Kennedy *et al.* [7]; \blacklozenge , Fedele *et al.* [21]; \ast , Bobbo *et al.* [22]; $+$, Daiguji and Hihara [23]; $-$, Wu and Yin [18]; $- - -$, Ihmels and Lemmon [1].

TOC/Abstract Graphic

